

pubs.acs.org/JACS Communication

# Creation and Reaction of Solvated Electrons at and near the Surface of Water

Xiao-Fei Gao, David J. Hood, Xianyuan Zhao, and Gilbert M. Nathanson\*



Cite This: J. Am. Chem. Soc. 2023, 145, 10987–10990



**Read Online** 

**ACCESS** I

III Metrics & More

Article Recommendations

S Supporting Information

**ABSTRACT:** Solvated electrons  $(e_s^-)$  are among nature's most powerful reactants, with over 2600 reactions investigated in bulk water. These electrons can also be created at and near the surface of water by exposing an aqueous microjet in vacuum to gas-phase sodium atoms, which ionize into  $e_s^-$  and  $Na^+$  within the top few layers. When a reactive surfactant is added to the jet, the surfactant and  $e_s^-$  become coreactants localized in the interfacial region. We report the reaction of  $e_s^-$  with the surfactant benzyltrimethylammonium in a 6.7 M LiBr/water microjet at 235 K and pH = 2. The reaction intermediates trimethylamine (TMA) and benzyl radical are identified by mass spectrometry after they evaporate from solution into the gas phase. Their detection demonstrates that TMA can escape before it is protonated and benzyl before it combines with itself or a H atom. Diffusion-reaction calculations indicate that  $e_s^-$  reacts on average within 20 Å of the surface and perhaps within the surfactant monolayer itself, while unprotonated TMA evaporates from the top 40 Å. The escape depth exceeds 1300 Å for the more slowly reacting benzyl radical. These proof-of-principle experiments establish an approach for exploring the near-interfacial analogues of aqueous bulk-phase radical chemistry through the evaporation of reaction intermediates into the gas phase.

C olvated electrons (e<sub>s</sub><sup>-</sup>) readily react with solutes in water due to their potent reduction potential and role as nucleophiles in breaking chemical bonds. Numerous studies have provided kinetic and mechanistic information for these e<sub>s</sub> reactions, along with parallel investigations of hydrogen atoms and hydroxyl radicals. <sup>1,2</sup> At the water—vapor interface of a surfactant-coated solution, however, e<sub>s</sub> may react differently because of its distinct solvation in an interfacial surfactant environment,3-5 followed by the escape of neutral reaction intermediates into the gas phase that would otherwise continue to react in the bulk. Our experiments complement those in bulk solution by probing reactions between e<sub>s</sub> and segregated solute molecules at and near the surface of water. This study follows earlier investigations of e<sub>s</sub> reactions near the surface of pure glycerol that generate evaporating hydrogen atomso and nonthermal electron reactions near the surface of pure methanol that generate dimethyl ether.

Several experimental approaches have been used to generate  $e_s^-$  in the near-interfacial region of liquid water. In pure water, photoionization produces transient and partially hydrated electrons at the air/water interface. Photoionization of the surface-active I<sup>-</sup> anion in water and ethanol also delivers solvated electrons near the surface. Adding the ionic surfactant tetrabutylammonium iodide enhances the surface concentration of I<sup>-</sup> and the solvated electrons released upon photoionization. Both experiment and theory indicate that these electrons rapidly become fully solvated and move below the surface. The recent innovation of atmospheric pressure plasmas has also enabled a steady source of solvated electrons reacting within the top 100 Å of solution.

Our group previously adopted sodium atom deposition and ionization to produce electrons near the glycerol-vacuum interface, limiting the reaction of solvated electrons within the

top ~50 Å.<sup>6</sup> Theoretically, molecular dynamics simulations predict that the Na 3s electron significantly delocalizes within 10 ps upon contact with glycerol<sup>17</sup> and within 1 ps with water.<sup>18</sup> Na atom hydrolysis has also been observed experimentally at the surface of amorphous ice.<sup>19</sup> These studies support the use of sodium atom ionization as a means to create transient, near-surface solvated electrons to explore chemical reactions.

In order to localize reactions of solvated electrons in the near-surface region, the reaction partner should also reside close to the surface. A natural approach is to choose a surfactant as the coreactant. Benzyltrimethylammonium  $([C_6H_5CH_2N(CH_3)_3]^+$ , BTMA<sup>+</sup>) is an ideal choice for the following reasons: first, BTMA+ is surface active in salty water, as described below. Second, BTMA+ reacts quickly with e<sub>s</sub>- to generate the benzyl radical  $(C_6H_5CH_2)$  and trimethylamine (TMA,  $(CH_3)_3N$ :) in water at  $\sim 2 \times 10^8/M/s$  at the 235 K temperature of our experiments (Table S2 of the Supporting Information),<sup>20</sup> thus enabling these reaction products to be generated in proximity to where the solvated electrons are initially born. Third, both benzyl and TMA are neutral species that can evaporate from solution and be probed by gas-phase detection methods. <sup>21,22</sup> Fourth, the reactions of TMA and benzyl in bulk solution provide internal clocks for determining their average depths before evaporation. In acidic solutions,

Received: March 31, 2023 Published: May 16, 2023





TMA is quickly protonated to TMAH<sup>+</sup>, suppressing evaporation. This protonation implies that any observable TMA in the gas-phase must have escaped before protonation occurs, thereby setting a characteristic depth for evaporating TMA. In addition, the benzyl radical can combine with itself or react with H atoms from  $H^+ + e_s^-$ , limiting the depth from which benzyl can evaporate (Sections S8 and S9).<sup>23</sup>

We describe experiments below demonstrating that e<sub>s</sub> reacts with BTMA+ close enough to the surface to generate benzyl radicals and TMA that escape into the gas phase. The average e<sub>s</sub> reaction depth is estimated to be only 20 Å, spanning a distance of roughly two BTMA+ molecules. This comparison suggests statistically that es may be reacting largely with BTMA+ in the surface region of the aqueous solution.

The experiments were conducted using a gas-microjet scattering apparatus in a vacuum (Figure S1).24 The experimental scheme is shown in Figure 1a. A beam of sodium

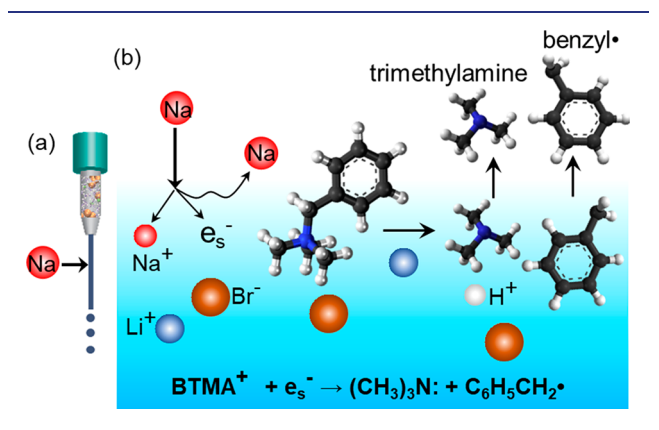


Figure 1. (a) Sodium atoms are directed at a 17  $\mu$ m radius microjet composed of 6.7 M LiBr and 0.25 M benzyltrimethylammonium (BTMA<sup>+</sup>) at pH = 2 and 235 K. (b) Na atoms ionize into Na<sup>+</sup> and  $e_s^$ in the near-surface region. These  $e_s^{\,-}$  can react with BTMA $^{\scriptscriptstyle +}$  at and near the surface to produce benzyl radical and trimethylamine, which may then evaporate before reacting in solution. H and H2 are also produced (from  $e_s^- + H^+ \rightarrow H$ ,  $e_s^- + H_2O \rightarrow H + OH^-$ , and H + H $\rightarrow$  H<sub>2</sub>) but were not monitored.

atoms from an oven is directed at a 17  $\mu$ m radius liquid jet in a vacuum at an average kinetic energy of 19 kJ/mol (Section S3). The aqueous microjet solution contains 6.7 M LiBr salt and 0.25 M BTMA<sup>+</sup> surfactant and is conditioned to pH  $\sim$  2 to suppress natural hydrolysis of BTMA+ by OH- (No TMA or benzyl is observed in the absence of Na atoms at pH = 2). The salty microjet is cooled to 235 K (0.1 Torr vapor pressure, 210 K freezing point) to minimize interference from evaporating water molecules colliding with the sodium atoms or evaporating reaction intermediates.<sup>24</sup> Liquid nitrogen cooled panels maintain the chamber pressure below  $1 \times 10^{-5}$  Torr. The jet travels at 14 m/s and is apertured to limit the observation region to 2.5-5.5 mm from the nozzle tip, corresponding to an observation time of 210  $\mu$ s. The jet is exposed to Na atoms over a longer time of 380 µs starting at the nozzle tip. Nonreacting sodium atoms (Section S4) and evaporating benzyl and TMA are chopped by a rotating wheel into 80  $\mu$ s packets that are ionized by electron impact and filtered by a quadrupole mass spectrometer. The arrival times of the mass-selected species are recorded as time-of-flight (TOF) spectra.

The equilibrium surface concentration of BTMA<sup>+</sup> was determined by surface tension measurements (Section S2) to be  $2 \times 10^{14}$ /cm<sup>2</sup> at 298 K for the 6.7 M LiBr/0.25 M BTMA<sup>+</sup> solution, corresponding to an average molecular area of 44 Å<sup>2</sup>. Although complete equilibration of the monolayer will not take place in the 170  $\mu$ s time for the solution to reach the beginning of the observation region at 2.5 mm, studies of tetrabutylammonium bromide in salty water imply that this time is sufficient for nearly complete diffusion and segregation of BTMA<sup>+</sup> (Section S2).<sup>25</sup> The reaction products we observe below suggest that these segregated BTMA+ ions pack loosely enough 26,27 to be porous and at least partly hydrated, such that Na atom ionization can occur within a region containing BTMA+, H2O, Br-, and Li+. Evidence that Na atoms do not always ionize in this environment comes from Figure 2, which

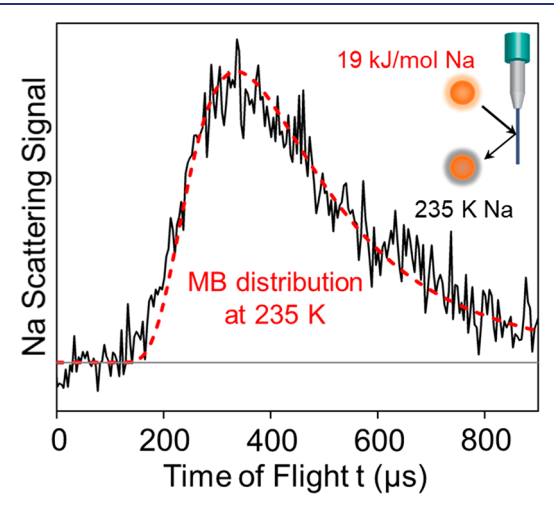


Figure 2. Time-of-flight spectrum of Na atoms following collisions with the microjet at an incident energy of 19 kJ/mol. The spectrum is fit well by a Maxwell-Boltzmann (MB) distribution at the 235 K jet temperature.

shows the TOF spectrum of impinging Na atoms scattered from the microjet. It is well-modeled by a Maxwell-Boltzmann distribution at the 235 K jet temperature, implying that these Na atoms dissipate their energy upon collision and then desorb in a thermal distribution before they fully ionize. We also find that some impinging Na atoms thermally desorb from the bare salty solution without surfactant. The escape probabilities of these Na atoms will be measured in future experiments.

The products of reaction between e<sub>s</sub> and BTMA<sup>+</sup> can also be observed upon exposing the microjet to Na atoms. Figure 3 shows the TOF spectrum of evaporating TMA. This spectrum closely mimics the Maxwell-Boltzmann distribution predicted for thermal evaporation of TMA molecules at 235 K. The slightly narrower arrival times likely arise from collisions of TMA with evaporating H<sub>2</sub>O within the water vapor cloud surrounding the jet.<sup>24,2</sup>

We also detected benzyl radical at the parent mass (m/z =91) with a similar intensity as TMA, as shown in Figure 4a. Three evaporating products may contribute to the m/z = 91signal recorded by the mass spectrometer: nascent benzyl radicals from the reaction of e<sub>s</sub> with BTMA+, toluene from reaction of benzyl and H, and bibenzyl from the selfcombination of benzyl radicals. Bibenzyl is ruled out because its heavier mass predicts much longer arrival times than are measured. However, toluene and benzyl cannot be distin-

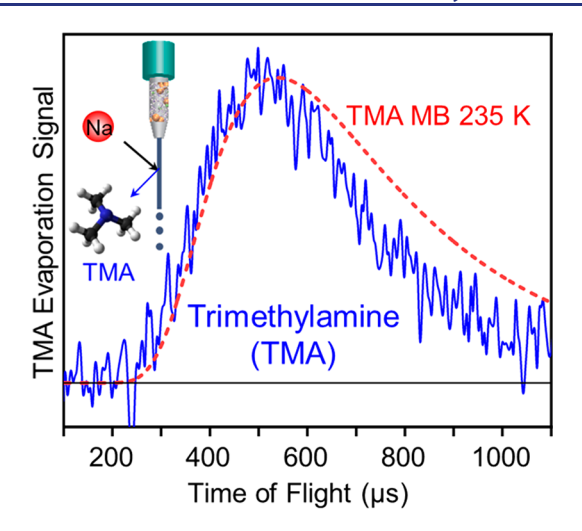
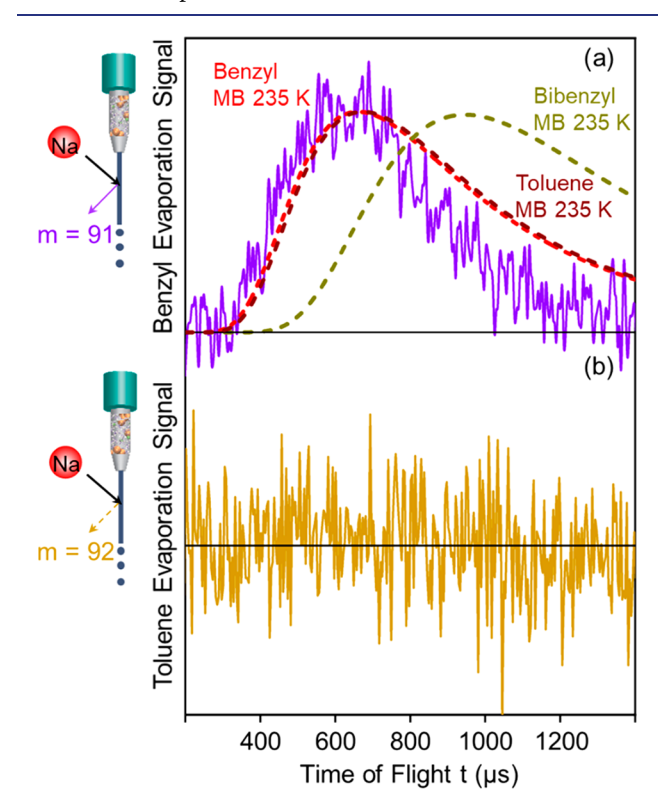


Figure 3. Time-of-flight spectrum of evaporating TMA measured at m/z = 58. A 235 K Maxwell–Boltzmann (MB) distribution for TMA is shown for comparison.



**Figure 4.** TOF spectra recorded at mass-to-charge ratio (m/z) (a) of 91 (benzyl) and (b) 92 (toluene). Maxwell-Boltzmann (MB) distributions of benzyl, toluene, and bibenzyl at 235 K are shown in panel (a) for comparison.

guished by their arrival times because of their similar masses. Unlike benzyl, toluene also ionizes significantly at its parent mass of m/z = 92. The flat spectrum in panel b, along with calibration spectra of pure toluene (Section S6), excludes toluene as the product. We therefore assign the m/z = 91spectrum to benzyl radicals that evaporate before reacting in solution.

To estimate where the observed TMA and benzyl radical originate in the jet solution, we calculate bulk-phase diffusionreaction depths for e<sub>s</sub> and the neutral species (TMA, benzyl, toluene, bibenzyl, H, and H<sub>2</sub>). These reactions include the production of TMA and benzyl from BTMA+ and their conversion into ionic (TMAH+) and evaporating neutral (toluene and bibenzyl) species. The full reaction scheme is shown in Figure S10. The concentration maps of each species generated by the diffusion-reaction equations are shown in Figure S11 as a function of exposure time and depth. Over the 380  $\mu$ s Na atom exposure window, the calculated average diffusion-reaction depths for  $e_s^-$ , TMA, and benzyl are 20  $\pm$ 10, 40  $\pm$  20, and 1300  $\pm$  600 Å, respectively (Section S9). These e<sub>s</sub> and TMA depths are small multiples of the ~11 and 3 Å sizes of BTMA+ and H2O. They are determined from diffusion-reaction calculations that incorporate bulk-phase diffusion and rate constants but not reactions with the monolayer itself. Within the 20 Å depth over which e<sub>s</sub> reacts, the number of BTMA+ in the surfactant layer outnumber those in this bulk-phase region by 7:1. This ratio suggests statistically that e<sub>s</sub> - encounters more segregated BTMA+ than bulk-phase BTMA+ and therefore e<sub>s</sub>- may react on average within the surfactant region itself.

TMA molecules that escape protonation evaporate on average from a 40 Å region at pH = 2, about twice as deep as their production from e<sub>s</sub><sup>-</sup> + BTMA<sup>+</sup>; these TMA molecules, perhaps produced within the surfactant region, then desorb immediately or diffuse over a shallow depth before evaporating. The absence of bibenzyl and toluene signals in Figure 4 is less effective in constraining the reaction region, as deduced from the larger 1300 Å average reaction depth for benzyl. This region is much deeper because the reaction partners for benzyl, either H or benzyl itself, are generated by es from the impinging Na atoms and are therefore dilute.

These initial experiments imply that e<sub>s</sub>-, generated from Na atoms, react with colocated surfactant molecules within tens of Angstroms of the surface to produce reaction intermediates that escape by evaporation rather than react further in solution. We hope that these experiments can ultimately provide a means to better distinguish between interfacial and subsurface reaction regions. In particular, lower pH solutions should compress the location of TMA protonation even closer to the surface, while systematic variations in surfactant concentration can discriminate between Langmuir-like surfactant and linear bulk-phase behavior. Our measurements further demonstrate that some Na atoms thermalize upon collision with the microjet but evaporate before they ionize, both in the absence and presence of surfactant. We are eager to learn how salt identity and surfactant packing control the ionization of Na atoms and reactivity of e<sub>s</sub> in close proximity to near-surface cations and anions, where electron-ion pairing may alter reactivity. 5,29,30 These future experiments will help reveal the range of reactivities exhibited by solvated electrons through the production of reaction intermediates at and near the surface of water and their escape into a vacuum.

### ASSOCIATED CONTENT

#### Supporting Information

The Supporting Information is available free of charge at https://pubs.acs.org/doi/10.1021/jacs.3c03370.

Discussions of experimental procedures, figures of gasmicrojet scattering apparatus, chemical structures, TOF spectra, surface tensions, mass spectra, scheme for bulkphase reactions initiated by e<sub>s</sub> in the microjet solution, concentration maps of time and depth, and concentration profiles, and tables of experimental and predicted

diffusion coefficients, predicted rate constants in 6.7 M LiBr/ $H_2O$  at 235 K, Henry's law constants and temperature coefficients, and characteristic depths for  $e_s^-$  and neutral species at 380  $\mu s$  (PDF)

## AUTHOR INFORMATION

#### **Corresponding Author**

Gilbert M. Nathanson — Department of Chemistry, University of Wisconsin-Madison, Madison, Wisconsin 53706, United States; orcid.org/0000-0002-6921-6841; Email: nathanson@chem.wisc.edu

### **Authors**

Xiao-Fei Gao – Department of Chemistry, University of Wisconsin-Madison, Madison, Wisconsin 53706, United States; orcid.org/0000-0002-9792-6218

David J. Hood — Department of Chemistry, University of Wisconsin-Madison, Madison, Wisconsin 53706, United States; ⊚ orcid.org/0000-0002-5895-9690

Xianyuan Zhao — Department of Chemistry, University of Wisconsin-Madison, Madison, Wisconsin 53706, United States; orcid.org/0000-0001-7926-6562

Complete contact information is available at: https://pubs.acs.org/10.1021/jacs.3c03370

#### Notes

The authors declare no competing financial interest.

#### ACKNOWLEDGMENTS

The authors thank the National Science Foundation for supporting this research under award number CHE-1900045.

# **■** REFERENCES

- (1) Buxton, G. V.; Greenstock, C. L.; Helman, W. P.; Ross, A. B. Critical-Review of Rate Constants for Reactions of Hydrated Electrons, Hydrogen-Atoms and Hydroxyl Radicals (·OH/·O<sup>-</sup>) In Aqueous-Solution. *J. Phys. Chem. Ref. Data* **1988**, *17*, 513–886.
- (2) Spinks, J. T.; Woods, R. J. An Introduction to Radiation Chemistry, 3rd ed.; Wiley: New York, 1990; Chapters 6 and 7.
- (3) Sagar, D. M.; Bain, C. D.; Verlet, J. R. R. Hydrated Electrons at the Water/Air Interface. J. Am. Chem. Soc. 2010, 132, 6917–6919.
- (4) Buchner, F.; Schultz, T.; Lubcke, A. Solvated Electrons at the Water-Air Interface: Surface versus Bulk Signal in Low Kinetic Energy Photoelectron Spectroscopy. *Phys. Chem. Chem. Phys.* **2012**, 14, 5837—5842
- (5) Karashima, S.; Suzuki, T. Charge-Transfer-to-Solvent Reaction in a Hydrophobic Tetrabutylammonium Iodide Molecular Layer in Aqueous Solution. *J. Phys. Chem. B* **2019**, 123, 3769–3775.
- (6) Alexander, W. A.; Wiens, J. P.; Minton, T. K.; Nathanson, G. M. Reactions of Solvated Electrons Initiated by Sodium Atom Ionization at the Vacuum-Liquid Interface. *Science* **2012**, 335, 1072–1075.
- (7) Chen, Z. W.; Li, Z. Y.; Hu, J.; Tian, S. X. Electron Impact with the Liquid-Vapor Interface. Acc. Chem. Res. 2022, 55, 3071-3079.
- (8) Siefermann, K. R.; Abel, B. The Hydrated Electron: A Seemingly Familiar Chemical and Biological Transient. *Angew. Chem., Int. Ed.* **2011**, *50*, 5264–5272.
- (9) Matsuzaki, K.; Kusaka, R.; Nihonyanagi, S.; Yamaguchi, S.; Nagata, T.; Tahara, T. Partially Hydrated Electrons at the Air/Water Interface Observed by UV-Excited Time-Resolved Heterodyne-Detected Vibrational Sum Frequency Generation Spectroscopy. *J. Am. Chem. Soc.* **2016**, *138*, 7551–7557.
- (10) Kondow, T.; Mafune, F. Structures and Dynamics of Molecules on Liquid Beam Surfaces. *Annu. Rev. Phys. Chem.* **2000**, *51*, 731.
- (11) Madarasz, A.; Rossky, P. J.; Turi, L. Excess Electron Relaxation Dynamics at Water/Air Interfaces. J. Chem. Phys. 2007, 126, 234707.

- (12) Uhlig, F.; Marsalek, O.; Jungwirth, P. Electron at the Surface of Water: Dehydrated or Not? *J. Phys. Chem. Lett.* **2013**, *4*, 338–343.
- (13) Nowakowski, P. J.; Woods, D. A.; Verlet, J. R. R. Charge Transfer to Solvent Dynamics at the Ambient Water/Air Interface. *J. Phys. Chem. Lett.* **2016**, *7*, 4079–4085.
- (14) Coons, M. P.; You, Z. Q.; Herbert, J. M. The Hydrated Electron at the Surface of Neat Liquid Water Appears To Be Indistinguishable from the Bulk Species. *J. Am. Chem. Soc.* **2016**, *138*, 10879–10886.
- (15) Herburger, A.; Barwa, E.; Oncak, M.; Heller, J.; van der Linde, C.; Neumark, D. M.; Beyer, M. K. Probing the Structural Evolution of the Hydrated Electron in Water Cluster Anions  $(H_2O)_n^-$ ,  $n \le 200$ , by Electronic Absorption Spectroscopy. *J. Am. Chem. Soc.* **2019**, *141*, 18000–18003.
- (16) Rumbach, P.; Bartels, D. M.; Sankaran, R. M.; Go, D. B. The Solvation of Electrons by an Atmospheric-Pressure Plasma. *Nat. Commun.* **2015**, *6*, 7248.
- (17) Wiens, J. P.; Nathanson, G. M.; Alexander, W. A.; Minton, T. K.; Lakshmi, S.; Schatz, G. C. Collisions of Sodium Atoms with Liquid Glycerol: Insights into Solvation and Ionization. *J. Am. Chem. Soc.* **2014**, *136*, 3065–3074.
- (18) Cwiklik, L.; Buck, U.; Kulig, W.; Kubisiak, P.; Jungwirth, P. A Sodium Atom in a Large Water Cluster: Electron Delocalization and Infrared Spectra. *J. Chem. Phys.* **2008**, *128*, 154306.
- (19) Kim, J. H.; Kim, Y. K.; Kang, H. Hydrolysis of Sodium Atoms on Water-Ice Films. Characterization of Reaction Products and Interfacial Distribution of Sodium and Hydroxide Ions. *J. Phys. Chem.* C **2009**, *113*, 321–327.
- (20) Bobrowski, K. Pulse-Radiolysis of Aqueous-Solutions of Benzyltrialkylammonium Cations Reactions with the Primary Transients from Water Radiolysis. *J. Phys. Chem.* **1981**, *85*, 382–388.
- (21) Leng, C. B.; Kish, J. D.; Roberts, J. E.; Dwebi, I.; Chon, N.; Liu, Y. Temperature-Dependent Henry's Law Constants of Atmospheric Amines. *J. Phys. Chem. A* **2015**, *119*, 8884–8891.
- (22) Staudinger, J.; Roberts, P. V. A Critical Review of Henry's Law Constants for Environmental Applications. *Crit. Rev. Environ. Sci. Technol.* **1996**, *26*, 205–297.
- (23) Mayouf, A. M.; Lemmetyinen, H.; Koskikallio, J. Self-Termination Rate of Parasubstituted Benzyl Radicals in Aqueous-Solutions A Time-Resolved Study. *J. Photochem. Photobiol., A* **1993**, 70, 215–221.
- (24) Gao, X. F.; Nathanson, G. M. Exploring Gas-liquid Reactions with Microjets: Lessons We are Learning. *Acc. Chem. Res.* **2022**, *55*, 3294–3302.
- (25) Sobyra, T. B.; Pliszka, H.; Bertram, T. H.; Nathanson, G. M. Production of  $Br_2$  from  $N_2O_5$  and  $Br^-$  in Salty and Surfactant-Coated Water Microjets. *J. Phys. Chem. A* **2019**, *123*, 8942–8953.
- (26) Lu, J. R.; Thomas, R. K.; Penfold, J. Surfactant Layers at the Air/Water Interface: Structure and Composition. *Adv. Colloid Interface Sci.* **2000**, *84*, 143–304.
- (27) Zhao, X. Y.; Nathanson, G. M.; Andersson, G. G. Experimental Depth Profiles of Surfactants, Ions, and Solvent at the Angstrom Scale: Studies of Cationic and Anionic Surfactants and Their Salting Out. J. Phys. Chem. B 2020, 124, 2218–2229.
- (28) Faubel, M.; Kisters, T. Non-Equilibrium Molecular Evaporation of Carboxylic-Acid Dimers. *Nature* **1989**, 339, 527–529.
- (29) Sauer, M. C.; Shkrob, I. A.; Lian, R.; Crowell, R. A.; Bartels, D. M.; Chen, X.; Suffern, D.; Bradforth, S. E. Electron Photodetachment from Aqueous Anions. 2. Ionic Strength Effect on Geminate Recombination Dynamics and Quantum Yield for Hydrated Electron. *J. Phys. Chem. A* **2004**, *108*, 10414–10425.
- (30) Narvaez, W. A.; Park, S. J.; Schwartz, B. J. Competitive Ion Pairing and the Role of Anions in the Behavior of Hydrated Electrons in Electrolytes. *J. Phys. Chem. B* **2022**, *126*, 7701–7708.